Supporting Information for “Thermodynamics of PtO_2 Superstructures on Pt”

7 References

1 Thermodynamics

We calculated Helmholtz free energies for Pt(111) and oxidized Pt(111) surface slabs (as defined in the main body and in chapter 2 of this Supporting Information) with respect to the ground state at 298 K and standard pressure in vacuum. Since the ΔPV of the stripes themselves per surface atom lies in the order of 10^{-5} eV – well within the individual differences between stripes, as we will show in chapter 6 of this Supporting information – we consider these Helmholtz free energies to be equal to the respective Gibbs free energies.

For oxygenation in a gaseous oxygen environment, the following reaction equation was used to define the formation energy of an oxidized surface with oxygen coverage y:

$$Pt(111) + \frac{y}{2}O_2(g) \rightarrow PtO_y/Pt(111) + Pt(em)$$

where $Pt(em)$ represents platinum atoms which are ejected from the surface oxide (allowing the oxide to “stretch” relative to the underlying surface).

From this reaction equation, the following formation energy is derived:

$$\Delta G_f\left(PtO_y/Pt(111)\right) = -\Delta G(Pt(111)) - \frac{y}{2}\Delta G\left(O_2(g)\right)$$

$$+ \Delta G\left(PtO_y/Pt(111)\right) + \Delta G(Pt(em))$$

in which the Pt(111)-based structure free energies are defined as $\Delta G(A) = E_{DFT}(A) + \Delta G_{vib}(A)$.

Similarly, the standard electrochemical potential $E^0(Pt_xO_y/Pt(111))$ is defined relative to the computational hydrogen electrode,[1] using half reaction equations

$$Pt(111) + y\,H_2O(l) \rightarrow PtO_y/Pt(111) + Pt(em) + 2y\,H^+ + 2y\,e^-$$

$$2\,H^+ + 2\,e^- \rightarrow H_2(g)$$

as

$$E^0\left(PtO_y/Pt(111)\right) = -\frac{1}{2y}\Delta G(Pt(111)) - \frac{1}{2}\Delta G\left(H_2O(l)\right)$$

$$+\frac{1}{2y}\Delta G\left(PtO_y/Pt(111)\right) + \frac{1}{2y}\Delta G(Pt(em)) + \frac{1}{2}\Delta G\left(H_2(g)\right).$$

$\Delta G\left(H_2(g)\right)$, $\Delta G\left(O_2(g)\right)$, and $\Delta G\left(H_2O(l)\right)$ are defined as described in chapter 3 of this Supporting Information. The value for $\Delta G(Pt(em))$ depends on the position in which the platinum atom is deposited; we assume the emitted atom is deposited in a surface island and sufficiently great numbers of atoms are emitted. If these assumptions hold, the step energy (at the island boundary) per emitted atom will converge to zero, effectively creating a new surface layer while stabilizing the underlying atoms – which means the effect of emitting the atom on the free energy is similar to inserting a new atom into the bulk. Hence, we assume $\Delta G(Pt(em)) = E_{bind}(Pt(s))$.

2 Computational details and stripe geometries

Table S.1. Cell Types, Unit Cell Dimensions and Associated *k* Point Grids

	M = $\sqrt{3}$		M = 2		M = 4	
Cell	Dimensions[a]	*k* grid	Dimensions[a]	*k* grid	Dimensions	*k* grid
Bulk (2×7×6)	–	–	$2d \times 7d \times 6d$	12 × 3 × 4	–	–
Bulk (2×8×6)	–	–	$2d \times 8d \times 6d$	12 × 3 × 4	–	–
Bulk (2×9×6)	–	–	$2d \times 9d \times 6d$	12 × 3 × 4	–	–
Bulk ($\sqrt{3}$×2$\sqrt{3}$×8)	$\sqrt{3}d \times 2\sqrt{3}d \times 8d$	14 × 7 × 3	–	–	–	–
Slab (M×3)	–	–	$2d \times 3d \times 25$ Å	12 × 8 × 1	–	–
Slab (M×4)	–	–	$2d \times 4d \times 25$ Å	12 × 6 × 1	$4d \times 4d \times 25$ Å	6 × 6 × 1
Slab (M×5)	–	–	$2d \times 5d \times 25$ Å	12 × 5 × 1	–	–
Slab (M×6)	–	–	$2d \times 6d \times 25$ Å	12 × 4 × 1	–	–
Slab (M×7)	–	–	$2d \times 7d \times 25$ Å	12 × 3 × 1	$4d \times 7d \times 25$ Å	6 × 3 × 1
Slab (M×8)	–	–	$2d \times 8d \times 25$ Å	12 × 3 × 1	$4d \times 8d \times 25$ Å	6 × 3 × 1
Slab (M×9)	–	–	$2d \times 9d \times 25$ Å	12 × 3 × 1	$4d \times 9d \times 25$ Å	6 × 3 × 1
Slab (M×10)	–	–	$2d \times 10d \times 25$ Å	12 × 3 × 1	–	–
Slab ($\sqrt{3}$×2$\sqrt{3}$)	$\sqrt{3}d \times 2\sqrt{3}d \times 25$ Å	14 × 7 × 1	–	–	–	–

a: d is the bulk shortest distance between atoms, i.e. $a/\sqrt{2}$.

3 Formation energies and DFT corrections for molecular species

$H_2(g)$ and $H_2O(l)$ Gibbs free energies were calculated by combining internal energies and vibrational zero point energies obtained using VASP with experimentally measured entropies and (for $H_2O(l)$) Gibbs energies of condensation in the CRC Handbook of Chemistry and Physics, as shown in Table S.2. For $O_2(g)$, however, the formation energy is hard to calculate due to the inaccuracy of spin-restricted PBE DFT with respect to simulating ground-state oxygen. Therefore, $\Delta G(O_2(g))$ has to be corrected using the respective free energies for $H_2(g)$ and $H_2O(l)$ and the formation energy of $H_2O(l)$ as obtained from the CRC Handbook.[5]

Table S.2. Formation Energies for Molecular Species

	E_{DFT} (eV)	E_{ZPE} (eV)	TS (eV)	pV (eV)	ΔG_{fus} (eV)	ΔG_{corr} (eV)	ΔG (eV)
$H_2(g)$	−6.767	0.270	0.404[a]	0.025	–	–	−6.926
$H_2O(l)$	−14.219	0.583	0.216[a]	0.025	−0.456[b]	–	−14.334
$O_2(g)$	−9.856	0.097	0.634[a]	–[b]	–	−0.493[b]	−9.899

a: Obtained from CRC Handbook.

b: Included in ΔG_{corr}.

c: Derived from calculated formation energies and $\Delta G_f(H_2O(l))$ obtained from CRC Handbook.

4. Bulk, surface and stripe vibrational analysis

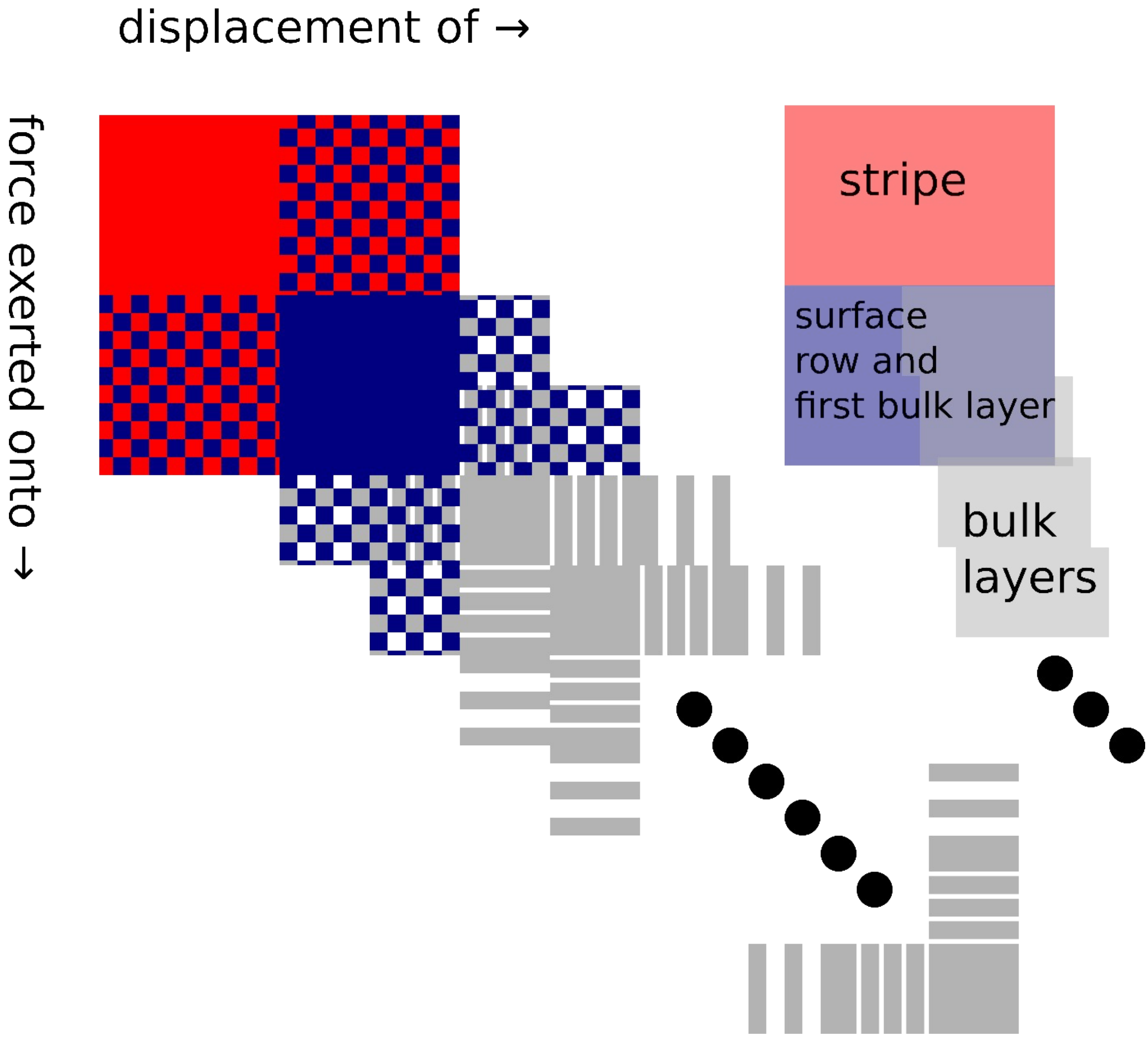

Figure S.1. A visualization of the Hessian matrices used to calculate the total system vibrational energies. Checkering and stripes indicate different coupling interactions. Red and blue domains were simulated in one single model and are kept separate to indicate the extent of coupling between surface and bulk single-atom displacement generated forces.

Reducing computational costs requires reducing the number of layers in each system without running into unphysical results such as negative force constants. For these stripe/bulk and stripe/surface systems, four layer stripe/surface simulations combined with corresponding eight layer bulk runs provided the precision required to obtain fewer than two negative eigenvalues for most stretching ratios. When we added fewer than three bulk layers, only positive eigenvalues were found. The results per set of atoms for each oxidized Pt system are listed in Table S.4.

Table S.4. Vibrational Energies for Selected Stripe Systems And Oxygenated Surfaces

								O* (ML)			
Layers	*Datasets*	2/3	5/6	6/7	7/8	8/9	4/4	0.25	0.33	0.67	1.00
Stripe only[a]	Stripe (meV)	–	422	445	464	478	579	–	–	–	–
	Surface (meV)	–	122	123	122	122	123	–	–	–	–
	ΔG_{vib} (meV)	**–**	**300**	**322**	**342**	**356**	**456**	**–**	**–**	**–**	**–**
+surface row	Stripe (meV)	458	572	595	615	630	734	353	372	540	676
	Surface (meV)	246	244	246	243	244	246	246	233	233	246
	ΔG_{vib} (meV)	**212**	**328**	**350**	**372**	**386**	**488**	**107**	**139**	**306**	**430**
+1 l	Stripe (meV)	747	852	876	895	912	1023	644	653	829	976
	Surface (meV)	488	538	544	538	538	515	515	513	513	515
	ΔG_{vib} (meV)	**260**	**314**	**332**	**358**	**373**	**508**	**130**	**140**	**316**	**461**
+2 l	Stripe (meV)	1045	1152	1176	1194	1213	1321	936	933	1110	1270
	Surface (meV)	783	838	844	837	839	812	812	795	795	812
	ΔG_{vib} (meV)	**262**	**314**	**332**	**358**	**374**	**508**	**124**	**138**	**315**	**458**
+3 l	Stripe (meV)										
	Surface (meV)										
	ΔG_{vib} (meV)										
+4 l	Stripe (meV)	1639	1755	1774	1787	1816	1910	1521	1494	1665	1858
	Surface (meV)	1380	1440	1445	1431	1442	1404	1404	1359	1359	1404
	ΔG_{vib} (meV)	**259**	**315**	**329**	**356**	**374**	**506**	**117**	**135**	**306**	**454**
+7 l	Stripe (meV)	2533	2660	2679	2681	2719	2801	2414	2343	2530	2743
	Surface (meV)	2276	2345	2347	2323	2346	2291	2291	2211	2211	2291
	ΔG_{vib} (meV)	**257**	**315**	**333**	**359**	**373**	**510**	**122**	**132**	**319**	**452**
+13 l	Stripe (meV)	4329	4470	4483	4466	4527	4576	4188	4045	4234	4516
	Surface (meV)	4076	4155	4151	4107	4154	4066	4066	3917	3917	4066
	ΔG_{vib} (meV)	**253**	**315**	**332**	**359**	**373**	**510**	**122**	**129**	**318**	**450**
+19 l	Stripe (meV)	6125	6280	6288	6250	6334	6351	5962	5751	5940	6290
	Surface (meV)	5873	5966	5955	5891	5961	5840	5840	5623	5623	5840
	ΔG_{vib} (meV)	**253**	**315**	**332**	**359**	**373**	**510**	**122**	**128**	**317**	**450**
+25 l	Stripe (meV)	7922	8091	8092	8035	8143	8126	7737	7457	7647	8065
	Surface (meV)	7669	7776	7760	7676	7769	7615	7615	7341	7341	7615
	ΔG_{vib} (meV)	**253**	**315**	**332**	**359**	**373**	**510**	**122**	**116**	**306**	**450**
+31 l	Stripe (meV)	9719	9901	9897	9819	9948	9901	9512	9163	9353	11615
	Surface (meV)	9466	9587	9564	9460	9575	9390	9390	9095	9095	11165
	ΔG_{vib} (meV)	**253**	**315**	**332**	**359**	**373**	**510**	**122**	**68**	**258**	**450**
+61 l	Stripe (meV)	18702	18990	18953	18919	18741	18775	18386	17694	17884	18714
	Surface (meV)	18449	18617	18639	18586	18383	18264	18264	17785	17785	18264
	ΔG_{vib} (meV)	**253**	**315**	**332**	**359**	**373**	**510**	**122**	**–91**	**99**	**450**
+91 l	Stripe (meV)	27685	28006	27941	27663	28029	27649	27261	26226	26415	27588
	Surface (meV)	27433	27691	27609	27305	27656	27139	27139	26317	26317	27139
	ΔG_{vib} (meV)	**253**	**315**	**332**	**359**	**373**	**510**	**122**	**–91**	**99**	**450**

a: Stripe energy equivalents for the surface are equal to half the vibrational free energy of a full surface layer.

The vibrational energy differences for all stretching ratios converge rapidly while adding additional layers. The differences between simulations with two additional bulk layers and three additional bulk layers are sufficiently small (~1 meV) to suggest convergence occurs around this third layer, which means that vibrational simulations are both converged and physical when one reaches this third bulk layer. Therefore, the +3l vibrational energies are used while calculating total (relative) formation energies.

Table S.4. Vibrational and Internal Energies for Selected Bulk Structures

	N = 6			*N* = 8	
Bulk structure[a]	E_{DFT}	G_{vib}	ΔG	E_{DFT}	G_{vib}
2 × 6 × *N*	−6.056	0.297	−5.759	−6.056	0.297
2 × 7 × *N*	−6.056	0.304	−5.752	−6.056	0.288
2 × 8 × *N*	−6.056	0.297	−5.759	−6.056	0.297
2 × 9 × *N*	−6.056	0.302	−5.754	−6.056	0.298

The mean energy of an emitted Pt atom is therefore 6.056 eV, with an error margin smaller than 0.001 eV. Vibrational free energies span 0.298±0.009 eV, while Gibbs free energies span −5.756±0.009 eV.

5 Formation energies of PtO_2 structures (standard conditions)

Table S.5. Energies of Most Stable 2×*N* PtO_2 Structures Per Stretching Ratio And On-Surface Oxygenated Pt(111)

Ratio[a]	$E_{DFT}(str)$	$E_{DFT}(surf)$	ΔE[b]	$G^0_{vib}(str)$	$G^0_{vib}(surf)$	$TS^0_{vib}(str)$	$TS^0_{vib}(surf)$	ΔG^0_f
2/3	−190.396	−173.947	**−0.401**	1.342	1.078	0.026	0.021	**−0.137**
3/4	−259.344	−259.344	**−0.434**	–	–	–	–	**–**
4/5	−328.453	−289.940	**−0.489**	–	–	–	–	**–**
5/6	−398.193	−327.897	**−0.546**	1.451	1.139	0.021	0.014	**−0.234**
6/7	−467.623	−405.901	**−0.578**	1.475	1.144	0.020	0.013	**−0.247**
7/8	−536.929	−463.865	**−0.596**	1.491	1.133	0.088	0.012	**−0.238**
8/9	−606.112	−521.897	**−0.599**	1.616	1.139	0.074	0.012	**−0.225**
9/10	−674.729	−579.888	**−0.575**	–	–	–	–	**–**
4/4	−275.453	−259.344	**−0.491**	1.615	1.108	0.022	0.013	**0.017**
0.25 ML O*	−244.201	−231.930	**−0.296**	1.229	1.108	0.022	0.013	**−0.175**
0.33 ML O*	−185.922	−173.970	**−0.342**	1.213	1.078	0.117	0.096	**−0.201**
0.67 ML O*	−196.454	−173.970	**−0.448**	1.388	1.078	0.120	0.096	**−0.132**
1.00 ML O*	−272.432	−231.930	**−0.114**	1.564	1.108	0.022	0.013	**0.341**

a: Energies are in eV; vibrational energies are derived from the top layer + 3 layer model as described in Chapter S.4.

b: Energy differences include rovibrational and translational free energies of O_2 and are expressed per surface atom

Table S.6. Energies of Most Stable Two 4×*N* PtO_2 Structures Per Stretching Ratio

Ratio[a]	$E_{DFT}(str)$	$E_{DFT}(surf)$	ΔE[b]	$\Delta E(stretched) - 2\Delta E(spaced)$
7/8	−1002.771	−927.763	**−0.614**	**−0.248**
8/9	−1130.526	−1043.839	**−0.615**	**−0.136**
4/4	−509.306	−463.860	**−0.491**	**−0.240**

a: *Energies are in eV.*

b: *Energy differences include rovibrational and translational free energies of O_2 and are expressed per surface atom.*

6 Stripe formation energies versus Pt binding energies

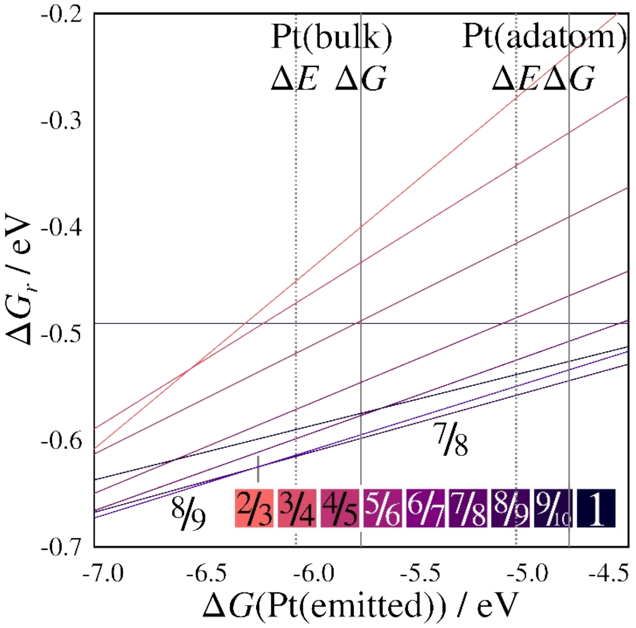

Figure S.2. Stripe formation energies (excluding vibrational energy contributions) with respect to emitted platinum binding energies.

1. Peterson, A. A.; Abild-Pedersen, F.; Studt, F.; Rossmeisl, J.; Norskov, J. K. How copper catalyzes the electroreduction of carbon dioxide into hydrocarbon fuels. *Energ Environ Sci* **2010,** *3* (9), 1311-1315.
2. Kresse, G.; Furthmuller, J. Efficient iterative schemes for ab initio total-energy calculations using a plane-wave basis set. *Phys Rev B* **1996,** *54* (16), 11169-11186.
3. Perdew, J. P.; Burke, K.; Ernzerhof, M. Generalized gradient approximation made simple. *Phys Rev Lett* **1996,** *77* (18), 3865-3868.
4. Hanselman, S.; Koper, M. T. M.; Calle-Vallejo, F. Computational Comparison of Late Transition Metal (100) Surfaces for the Electrocatalytic Reduction of CO to C-2 Species. *Acs Energy Lett* **2018,** *3* (5), 1062-1067.
5. Lide, D. R. *CRC Handbook of Chemistry and Physics, 84th Edition*. CRC Press: 2003.